A new type of optical heterodyne polarimeter

2003 Meas. Sci. Technol. 14 55

(http://iopscience.iop.org/0957-0233/14/1/308)

INSTITUTE OF PHYSICS PUBLISHING MEASUREMENT SCIENCE AND TECHNOLOGY
Meas. Sci. Technol. **14** (2003) 55–58 PII: S0957-0233(03)37209-1

A new type of optical heterodyne polarimeter

Jiun-You Lin and Der-Chin Su

Institute of Electro-Optical Engineering, National Chiao Tung University,
1001 Ta-Hsueh Road, Hsin-Chu 300, Taiwan, Republic of China

E-mail: t7503@faculty.nctu.edu.tw (D-C Su)

Received 21 May 2002, in final form 29 October 2002, accepted for publication 5 November 2002
Published 26 November 2002
Online at stacks.iop.org/MST/14/55

Abstract
Phase variations occur when a circularly polarized light beam either passes through a chiral solution or is reflected from a non-absorbing material. They can be measured accurately with a circular heterodyne interferometry. These data are substituted into the special equations derived from Jones calculus. The chiral parameter and the average refractive index of a chiral solution can be estimated simultaneously in just one optical configuration. This polarimeter has the merits of both the common-path interferometer and the heterodyne interferometer. The proposed device was validated in this work.

Keywords: chiral parameter, refractive index, heterodyne interferometry, standards and calibration

1. Introduction

A chiral solution is often used in biological technology, medicine, and pharmaceutics [1, 2]. Its chiral parameter and average refractive index are very important characteristics for the understanding of its quantum structure and geometric configuration [3].

Polarimeters are commonly used to measure the chiral parameter. This is related to the measurement of light intensity variations [4]. Thus, the stability of the light source, the scattering light, and the internal reflections influence the measurement accuracy. Chou *et al* [5, 6] presented a heterodyne polarimeter by introducing the heterodyne interferometry into a Mach–Zehnder interferometric configuration. Because of its two-path optical configuration, it is susceptible to air turbulence and it can become unstable. Other methods for measuring the average refractive index have been presented based on the effect of either the total internal reflection [7] or Brewster angle [8]. These methods produced good measurement results. To the author's knowledge, there is no reference reported for measuring the chiral parameter and the average refractive index simultaneously in one optical configuration. To improve on this, a new type of optical heterodyne polarimeter is presented in this paper. It has the merits of both the common-path interferometer and the hereodyne interferometer.

2. Principles [8, 9, 10]

Figure 1 schematically illustrates the improved optical heterodyne polarimeter. For convenience, the $+z$-axis is chosen to be along the light propagation direction and the x-axis is along the direction perpendicular to the paper plane. A light coming from a heterodyne light source having an angular frequency difference ω between s- and p-polarizations passes through a quarter-waveplate Q. If the fast axis of Q is located at 45° to the x-axis, then the Jones vector of the light can be written as

$$E_i = \frac{1}{2}\begin{pmatrix}1\\ \mathrm{i}\end{pmatrix}\exp\left(\mathrm{i}\frac{\omega t}{2}\right) + \frac{1}{2}\begin{pmatrix}1\\ -\mathrm{i}\end{pmatrix}\exp\left(-\mathrm{i}\frac{\omega t}{2} + \mathrm{i}\frac{\pi}{2}\right). \quad (1)$$

From equation (1), we can see that the right- and the left-circular polarizations have frequency shifts $\omega/2$ and $-\omega/2$, respectively. Thus there is an angular frequency difference ω between them. The light is incident on a beam splitter BS, and is divided into two parts: the reflected light and the transmitted light. The reflected light passes through an analyser AN_r and enters a photodetector D_r. If the transmission axis of AN_r is located at 45° to the x-axis, then the Jones vector of the light arriving at D_r is

$$E_r = \frac{1}{2}\begin{pmatrix}1 & 1\\ 1 & 1\end{pmatrix}\begin{pmatrix}\exp\left(-\mathrm{i}\frac{\phi_{BS}}{2}\right) & 0\\ 0 & \exp\left(\mathrm{i}\frac{\phi_{BS}}{2}\right)\end{pmatrix}$$

$$\times \frac{1}{2}\left[\begin{pmatrix}1\\ \mathrm{i}\end{pmatrix}\exp\left(\mathrm{i}\frac{\omega t}{2}\right)+\begin{pmatrix}1\\ -\mathrm{i}\end{pmatrix}\exp\left(-\mathrm{i}\frac{\omega t}{2}+\mathrm{i}\frac{\pi}{2}\right)\right]$$
$$=\frac{1}{4}\left[\left(\mathrm{i}\exp\left(\mathrm{i}\frac{\phi_{BS}}{2}\right)+\exp\left(-\mathrm{i}\frac{\phi_{BS}}{2}\right)\right)\right.$$
$$\times\ \exp\left(\mathrm{i}\frac{\omega t}{2}\right)+\left(\mathrm{i}\exp\left(-\mathrm{i}\frac{\phi_{BS}}{2}\right)\right.$$
$$\left.\left.+\ \exp\left(\mathrm{i}\frac{\phi_{BS}}{2}\right)\right)\exp\left(-\mathrm{i}\frac{\omega t}{2}\right)\right]\begin{pmatrix}1\\ 1\end{pmatrix}. \quad (2)$$

The intensity measured by D_r is

$$I_r = |E_r|^2 = \tfrac{1}{2}(1+2\cos\phi_{BS}\cos\omega t), \quad (3)$$

where I_r is the reference signal and ϕ_{BS} is the phase difference between p- and s-polarizations produced by the reflection at BS. On the other hand, the transmitted light enters a rectangular glass box containing the chiral solution with the average refractive index n and the chiral parameter g, and a transparent glass plate G with the refractive index n_g inclined against the wall of the glass box at 45°, as shown in figure 2. Here the chiral parameter is defined as [11]

$$g = \frac{n_l - n_r}{2}, \quad (4)$$

where n_l and n_r denote the refractive indices of the left- and the right-circular polarizations, respectively. After the light propagates a distance d in the chiral solution, its Jones vector can be written as

$$E_i' = \frac{1}{2}\begin{pmatrix}1\\ \mathrm{i}\end{pmatrix}\exp\left(\mathrm{i}\frac{\omega t}{2}-\mathrm{i}k_r d\right)$$
$$+\frac{1}{2}\begin{pmatrix}1\\ -\mathrm{i}\end{pmatrix}\exp\left(-\mathrm{i}\frac{\omega t}{2}+\mathrm{i}\frac{\pi}{2}-\mathrm{i}k_l d\right), \quad (5)$$

where k_l and k_r represent the wavenumbers of the left- and the right-circular polarizations, respectively. Then the light is divided again into two parts by the glass plate G: the reflected light and the transmitted light. They propagate distances d_1 and d_2 in the chiral solution, pass through analysers AN_1 and AN_2 and enter photodetectors D_1 and D_2, respectively. Let r and t be the reflection coefficient and the transmission coefficient at the interface as the light from the chiral solution is incident on the glass plate G, t' be the transmission coefficient at the interface as the light from the glass plate G is incident on the chiral solution, and subscripts p and s denote p-and s-polarizations, respectively. If both the transmission axes of AN_1 and AN_2 are located at 45° to the x-axis, then the Jones vectors of the light arriving D_1 and D_2 become

$$E_1 = \frac{1}{2}\begin{pmatrix}1 & 1\\ 1 & 1\end{pmatrix}\begin{pmatrix}\cos\theta_1 & -\sin\theta_1\\ \sin\theta_1 & \cos\theta_1\end{pmatrix}\begin{pmatrix}r_p & 0\\ 0 & r_s\end{pmatrix}$$
$$\times\left[\frac{1}{2}\begin{pmatrix}1\\ \mathrm{i}\end{pmatrix}\exp\left(\mathrm{i}\frac{\omega t}{2}-\mathrm{i}k_r d\right)\right.$$
$$\left.+\frac{1}{2}\begin{pmatrix}1\\ -\mathrm{i}\end{pmatrix}\exp\left(-\mathrm{i}\frac{\omega t}{2}+\mathrm{i}\frac{\pi}{2}-\mathrm{i}k_l d\right)\right]$$
$$=\frac{1}{4}A\left[\exp\left(\mathrm{i}\frac{\omega t}{2}-\mathrm{i}k_r d+\mathrm{i}\phi_1\right)\right.$$
$$\left.+\ \exp\left(-\mathrm{i}\frac{\omega t}{2}-\mathrm{i}k_l d-\mathrm{i}\phi_1+\mathrm{i}\frac{\pi}{2}\right)\right]\begin{pmatrix}1\\ 1\end{pmatrix}, \quad (6)$$

and

$$E_2 = \frac{1}{2}\begin{pmatrix}1 & 1\\ 1 & 1\end{pmatrix}\begin{pmatrix}\cos\theta_2 & -\sin\theta_2\\ \sin\theta_2 & \cos\theta_2\end{pmatrix}\begin{pmatrix}t_p' & 0\\ 0 & t_s'\end{pmatrix}\begin{pmatrix}t_p & 0\\ 0 & t_s\end{pmatrix}$$
$$\times\left[\frac{1}{2}\begin{pmatrix}1\\ \mathrm{i}\end{pmatrix}\exp\left(\mathrm{i}\frac{\omega t}{2}-\mathrm{i}k_r d\right)\right.$$
$$\left.+\frac{1}{2}\begin{pmatrix}1\\ -\mathrm{i}\end{pmatrix}\exp\left(-\mathrm{i}\frac{\omega t}{2}+\mathrm{i}\frac{\pi}{2}-\mathrm{i}k_l d\right)\right]$$
$$=\frac{1}{4}B\left[\exp\left(\mathrm{i}\frac{\omega t}{2}-\mathrm{i}k_r d+\mathrm{i}\phi_2\right)\right.$$
$$\left.+\ \exp\left(-\mathrm{i}\frac{\omega t}{2}-\mathrm{i}k_l d-\mathrm{i}\phi_2+\mathrm{i}\frac{\pi}{2}\right)\right]\begin{pmatrix}1\\ 1\end{pmatrix}, \quad (7)$$

respectively, where

$$A = \sqrt{[r_p(\cos\theta_1+\sin\theta_1)]^2+[r_s(\cos\theta_1-\sin\theta_1)]^2}, \quad (8)$$

$$\phi_1 = \tan^{-1}\left[\frac{r_s(\cos\theta_1-\sin\theta_1)}{r_p(\cos\theta_1+\sin\theta_1)}\right], \quad (9)$$

$$\theta_1 = (k_r-k_l)d_1 = \frac{2\pi}{\lambda}(n_r-n_l)d_1, \quad (10)$$

$$r_p = \frac{n'^2-\sqrt{2n'^2-1}}{n'^2+\sqrt{2n'^2-1}}, \quad (11)$$

$$r_s = \frac{1-\sqrt{2n'^2-1}}{1+\sqrt{2n'^2-1}}, \quad (12)$$

$$B = \sqrt{[t_p t_p'(\cos\theta_2+\sin\theta_2)]^2+[t_s t_s'(\cos\theta_2-\sin\theta_2)]^2}, \quad (13)$$

$$\phi_2 = \tan^{-1}\left[\frac{t_s t_s'(\cos\theta_2-\sin\theta_2)}{t_p t_p'(\cos\theta_2+\sin\theta_2)}\right], \quad (14)$$

$$\theta_2 = (k_r-k_l)d_2 = \frac{2\pi}{\lambda}(n_r-n_l)d_2, \quad (15)$$

$$t_p = \frac{1}{n'}(r_p+1), \quad (16)$$

$$t_s = r_s+1, \quad (17)$$

$$t_p' = \frac{2n''\cos\alpha}{n''^2\cos\alpha+\sqrt{n''^2-\sin^2\alpha}}, \quad (18)$$

$$t_s' = \frac{2\cos\alpha}{\cos\alpha+\sqrt{n''^2-\sin^2\alpha}}, \quad (19)$$

$$\alpha = \sin^{-1}\left(\frac{1}{\sqrt{2}n'}\right), \quad (20)$$

$n' = n_g/n$, and $n'' = (n')^{-1}$. Consequently the intensities measured by D_1 and D_2 are

$$I_1 = |E_1|^2 = \tfrac{1}{8}A^2[1+\cos(\omega t+\psi_1)], \quad (21)$$

and

$$I_2 = |E_2|^2 = \tfrac{1}{8}B^2[1+\cos(\omega t+\psi_2)], \quad (22)$$

where

$$\psi_1 = 2\phi_1+\phi-\frac{\pi}{2}, \quad (23)$$

$$\psi_2 = 2\phi_2+\phi-\frac{\pi}{2}, \quad (24)$$

and

$$\phi = (k_l-k_r)d = \frac{2\pi}{\lambda}(n_l-n_r)d = \frac{4\pi}{\lambda}gd. \quad (25)$$

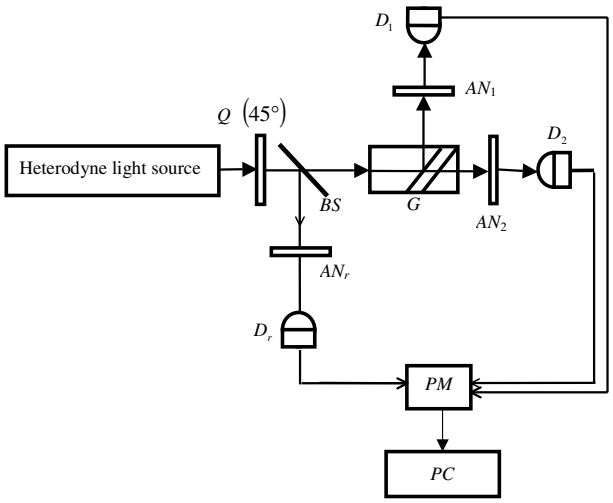

Figure 1. Schematic illustration of the new type of optical heterodyne polarimeter, BS: beam splitter, PM: phase meter; AN: analyser; D: detector; PC: personal computer.

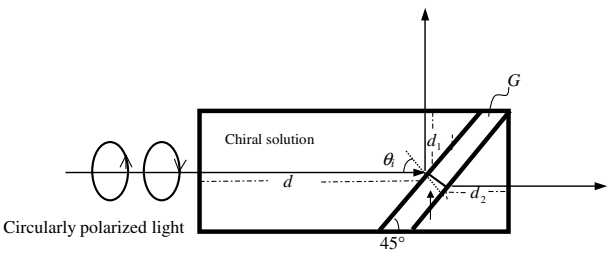

Figure 2. Schematic illustration of the glass box containing the chiral solution and a glass plate G.

Two pairs of signals (I_r, I_1) and (I_r, I_2) are sent to a phase meter PM. Their phase differences ψ_1 and ψ_2 are obtained.

From equations (9)–(12), (14)–(20) and (25), it is obvious that ψ_1 and ψ_2 are the functions of n, g, d, d_1, d_2 and n_g. ψ_1 and ψ_2 can be experimentally measured under the condition that d, d_1, d_2, and n_g are specified. Hence a set of simultaneous equations

$$\psi_1 = \psi_1(n, g), \tag{26}$$

$$\psi_2 = \psi_2(n, g), \tag{27}$$

are obtained. These simultaneous equations are solved using the Runge–Kutta method [12], where the parameters n and g can be estimated.

3. Experiments and results

In order to show the feasibility of this method, we measured the average refractive indices and the chiral parameters of glucose solutions and sucrose solutions at 20 °C. The heterodyne light source [8] consisting of a He–Ne laser with a wavelength of 632.8 nm and an electro-optic modulator was used. The frequency difference between the left- and right-circular polarizations was 1 kHz. A quartz glass plate with a refractive index 1.4570 was inserted into the chiral solution, and d, d_1, and d_2 were 50, 10 and 10 mm, respectively. The rectangular glass box containing the test chiral solution and the glass plate G was mounted on a high-precision rotation stage (model M-URM100PP, Newfocus) with an angular resolution of 0.001°. A phase meter with resolution 0.01° was self-made. In addition, a personal computer was employed to record and analyse the data. The experimental results and their corresponding reference values are summarized in table 1, where g_{ref} is derived from the reference values and the definition of the specific rotation [1, 13]. It is clear that they show good agreement.

4. Discussion

From equation (25) we get

$$|\Delta g| = \left|\frac{\lambda}{4\pi d}\right||\Delta\phi| + \left|\frac{\lambda\phi}{4\pi d^2}\right||\Delta d|, \tag{28}$$

where Δg, $\Delta\phi$ and Δd are the errors of g, ϕ and d, respectively. Considering the angular resolution of the phase meter, the second-harmonic error and the polarization-mixing error, $|\Delta\phi| \cong 0.03°$ can be estimated in our experiments [14]. In addition, the condition $|\Delta d| = 0.01$ mm is also assumed in our experiments. Substituting these data and the experimental conditions into equation (28) gives $|\Delta g| \cong 5.5 \times 10^{-10}$.

From equations (23) and (24), we have

$$\begin{aligned}\psi' = \psi_2 - \psi_1 &= 2\tan^{-1}\left[\frac{t_s t_s'(\cos\theta_2 - \sin\theta_2)}{t_p t_p'(\cos\theta_2 + \sin\theta_2)}\right] \\ &\quad - 2\tan^{-1}\left[\frac{r_s(\cos\theta_1 - \sin\theta_1)}{r_p(\cos\theta_1 + \sin\theta_1)}\right] \\ &= 2\tan^{-1}(((\cos\theta_2 - \sin\theta_2)(\cos\theta_1 + \sin\theta_1)r_p t_s t_s' \\ &\quad - (\cos\theta_1 - \sin\theta_1)(\cos\theta_2 + \sin\theta_2)r_s t_p t_p') \\ &\quad \times ((\cos\theta_2 + \sin\theta_2)(\cos\theta_1 + \sin\theta_1)r_p t_p t_p' \\ &\quad + (\cos\theta_2 - \sin\theta_2)(\cos\theta_1 - \sin\theta_1)r_s t_s t_s')^{-1}).\end{aligned} \tag{29}$$

From equation (29), we obtain

$$\Delta n \cong \left.\frac{|\sec^2(\frac{\psi'}{2})\Delta\psi'| + |\frac{\partial h}{\partial\theta_i}\Delta\theta_i| + |\frac{\partial h}{\partial\theta_1}\Delta\theta_1| + |\frac{\partial h}{\partial\theta_2}\Delta\theta_2|}{|\frac{\partial h}{\partial n}|}\right|_{\theta_i=45°}, \tag{30}$$

where Δn, $\Delta\psi'$, $\Delta\theta_i$, $\Delta\theta_1$ and $\Delta\theta_2$ are the errors of n, ψ', θ_i, θ_1 and θ_2, respectively.

In the above equation, $|\Delta\theta_1|$, $|\Delta\theta_2|$, and h can be expressed as

$$|\Delta\theta_1| = \left|\frac{4\pi}{\lambda}(n_r - n_l)\Delta d_1\right| = \left|\frac{4\pi}{\lambda}g\Delta d_1\right|, \tag{31}$$

$$|\Delta\theta_2| = \left|\frac{4\pi}{\lambda}(n_r - n_l)\Delta d_2\right| = \left|\frac{4\pi}{\lambda}g\Delta d_2\right|, \tag{32}$$

and

$$\begin{aligned}h &= h(n, \theta_i, \theta_1, \theta_2) \\ &= \left.\frac{m_1 n_2 r_p(\theta_i)t_s(\theta_i)t_s'(\theta_i) - n_1 m_2 r_s(\theta_i)t_p(\theta_i)t_p'(\theta_i)}{m_1 m_2 r_p(\theta_i)t_p(\theta_i)t_p'(\theta_i) + n_1 n_2 r_s(\theta_i)t_s(\theta_i)t_s'(\theta_i)}\right|_{\theta_i=45°},\end{aligned} \tag{33}$$

respectively; where

$$m_1 = \cos\theta_1 + \sin\theta_1, \tag{34}$$

$$n_1 = \cos\theta_1 - \sin\theta_1, \tag{35}$$

$$m_2 = \cos\theta_2 + \sin\theta_2, \tag{36}$$

Table 1. Experimental results and the corresponding reference data.

Solutions	ψ_1 (deg)	ψ_2 (deg)	$g(\times 10^8)$	$g_{ref}(\times 10^8)$ (at 632.8 nm)	n	n_{ref} (at 589.3 nm)
Glucose ($w = 5\%$)	−258.84	2.44	4.07	4.01[a]	1.3394	1.3402[b]
Glucose ($w = 10\%$)	−257.12	5.31	8.22	8.17[a]	1.3472	1.3477[b]
Sucrose ($w = 5\%$)	−258.25	3.18	5.16	5.11[c]	1.3396	1.3403[b]
Sucrose ($w = 10\%$)	−256.01	6.77	10.35	10.43[c]	1.3483	1.3478[b]

[a] Reference [1].
[b] Reference [13].
[c] Estimated data from [13] with a curve fitting technique.

$$n_2 = \cos\theta_2 - \sin\theta_2, \tag{37}$$

$$r_p(\theta_i) = \frac{n'^2\cos\theta_i - \sqrt{n'^2 - \sin^2\theta_i}}{n'^2\cos\theta_i + \sqrt{n'^2 - \sin^2\theta_i}}, \tag{38}$$

$$r_s(\theta_i) = \frac{\cos\theta_i - \sqrt{n'^2 - \sin^2\theta_i}}{\cos\theta_i + \sqrt{n'^2 - \sin^2\theta_i}}, \tag{39}$$

$$t_p(\theta_i) = \frac{1}{n'}[r_p(\theta_i) + 1], \tag{40}$$

$$t_s(\theta_i) = r_s(\theta_i) + 1, \tag{41}$$

$$t'_p(\theta_i) = \frac{2n''\cos\alpha}{n''^2\cos\alpha + \sqrt{n''^2 - \sin^2\alpha}}, \tag{42}$$

$$t'_s(\theta_i) = \frac{2\cos\alpha}{\cos\alpha + \sqrt{n''^2 - \sin^2\alpha}}, \tag{43}$$

$$\alpha = \sin^{-1}\left(\frac{\sin\theta_i}{n'}\right). \tag{44}$$

Substituting our experimental conditions $|\Delta\psi'| \cong 0.03°$, $|\Delta\theta_i| = 0.001°$, $|\Delta d_1| = |\Delta d_2| = 0.01$ mm and the measured values of n and g of each test chiral solution into equation (30) yields $|\Delta n| \cong 5 \times 10^{-4}$.

From equations (8), (11), (12) and (21) it can be seen that the signal I_1 is too weak to be measured, as n' is nearly equal to one. To avoid this drawback, the refractive index of the glass plate G should be chosen so that it is different from the average index of the chiral solution under test. A beam-splitting cube can divide the incident light into two parts, the reflected light and the transmitted light, as the glass plate G does. But because the reflective thin film in the beam-splitting cube does not contact with the test chiral solution, its reflected light is independent to the average refractive index of the test chiral solution. Hence a beam-splitting cube cannot be introduced to our experimental setup to replace the glass plate G.

If the function generator is used to generate the electrical reference signal, then the optical setup can be simplified [8]. Note, however, that the reference signal is influenced by the electronic noise and the data of $\Delta\phi$ will fluctuate. In our experiments, both the reference signal and the test signal are affected by the electronic noise. Their fluctuations tend to cancel out such that the data of $\Delta\phi$ can be read directly in a stable manner.

5. Conclusions

Phase variations occur when a circularly polarized light beam either passes through a chiral solution or is reflected from non-absorbing materials. They can be measured accurately with circular heterodyne interferometry. The chiral parameter and the average refractive index of a chiral solution can be measured simultaneously in just one optical configuration. Because of the common-path configuration and heterodyne phase measurement, this polarimeter has the merits of simple structure, easy operation, rapid measurement and high stability. The prototype was set up to demonstrate its validity. The estimated accuracy of the chiral parameters for the glucose or sucrose solutions is 5.5×10^{-10}, and the estimated accuracy of the average refractive index is 5×10^{-4}.

Acknowledgment

This study was supported in part by the National Science Council, Taiwan, Republic of China, under contract no NSC 90-2215-E-009-077.

References

[1] McNicols R J and Cote G L 2000 *J. Biomed. Opt.* **5** 5
[2] Yang P K and Huang J Y 1998 *J. Opt. Soc. Am.* B **15** 1698
[3] Silverman M P, Ritchie N, Cushman G M and Fisher B 1988 *J. Opt. Soc. Am.* **5** 1852
[4] King T W, Cote G L, McNichols R and Goetz M K Jr 1994 *Opt. Eng.* **33** 2746
[5] King H J, Chou C, Chang H and Huang Y C 1994 *Opt. Commun.* **110** 259
[6] Chou C, Huang Y C, Feng C M and Chang M 1997 *Japan. J. Appl. Phys.* **36** 356
[7] Chou M H, Lee J Y and Su D C 1997 *Appl. Opt.* **36** 2936
[8] Lee J Y and Su D C 1998 *J. Opt.* **29** 349
[9] Caldwell D J and Eyring H 1971 *The Theory of Optical Activity* (New York: Wiley) ch 1
[10] Huard S 1997 *Polarization of Light* (New York: Wiley) ch 5
[11] Silverman M P and Badoz J 1992 *J. Electromagn. Wave Appl.* **6** 587
[12] Koomin S E and Meredith D C 1990 *Computational Physics* (Reading, MA: Addison-Wesley) ch 2
[13] Weast R C (ed) 1981 *CRC Handbook of Chemistry and Physics* 61st edn (Boca Raton, FL: Chemical Rubber Company Press) pp D227–70, E-418
[14] Chiu M H, Lee J Y and Su D C 1999 *Appl. Opt.* **38** 4047